

# DECONFINEMENT OF QUARKS AND GLUONS IN NUCLEUS-NUCLEUS COLLISIONS

M.I. GORENSTEIN

Bogolyubov Institute for Theoretical Physics, Nat. Acad. of Sci. of Ukraine  
(14b, Metrolohichna Str., Kyiv 03680, Ukraine)

PACS 12.38.Mh, 25.75.Dw  
©2011

The energy dependence of hadron production in relativistic nucleus-nucleus collisions reveals the anomalies. They were predicted as the signals of the deconfinement phase transition and observed by NA49 collaboration in Pb+Pb collisions at the CERN SPS. This indicates the onset of the deconfinement in central nucleus-nucleus collisions at about 30 AGeV.

## 1. Introduction

What are the phases of strongly interacting matter and what do the transitions between them look like? These questions motivate broad experimental and theoretical efforts since more than 40 years. In particular, the advent of the quark model of hadrons and the development of the commonly accepted theory of strong interactions, quantum chromodynamics, naturally led to expectations that matter at very high densities may exist in a state of quasifree quarks and gluons, the quark-gluon plasma (QGP) [1–3].

Experimental searches for QGP signals started at the Super Proton Synchrotron (SPS) of the European Organization for Nuclear Research (CERN) and the Alternating Gradient Synchrotron (AGS) of Brookhaven National Laboratory (BNL) in the mid-1980s. Today they are pursued also at much higher collision energies at the Relativistic Heavy Ion Collider (RHIC) at BNL. The experiments on nucleus-nucleus (A+A) collisions at the Large Hadron Collider (LHC) in CERN join the world efforts at energies 20 times higher than those at RHIC. It is most probably that the QGP is formed at the early stage of heavy ion collisions at the top SPS energy and at RHIC energies. The unambiguous evidence of the QGP state was however missing. This may be attributed to the difficulty of obtaining the unique and quantitative predictions of expected QGP signals from the theory of strong interactions. For this reason, the NA49 Collaboration at the CERN SPS has searched over the past years for signs of the onset of QGP creation in the energy dependence of hadron production properties. This search was motivated by the statistical model

of the early stage (SMES) [4], showing that the onset of deconfinement should lead to rapid changes of the energy dependence of numerous experimentally detectable properties of the collisions, all appearing in a common energy domain. The energy scan program of the NA49 Collaboration recorded central Pb+Pb collisions at several energies: 20, 30, 40, 80, and 158 AGeV [5]. The predicted features have been observed, and new experiments now continue detailed studies in the energy region of the onset of deconfinement. In this paper, we review the experimental and theoretical status of the onset of deconfinement (more details can be found in [6]). The basic qualitative ideas are presented, and the SMES signals of deconfinement are discussed and compared with the latest experimental results.

## 2. Kink

It is natural to expect that, as the collision energy increases, the energy density at the early stage of A+A collisions also increases. We may hope that, with increase in the collision energy, we can detect anomalies in the energy dependence of hadron production properties and thus discover successive transitions between various phases of a strongly interacting matter created at the early stage of collisions. At a sufficiently high collision energy, the matter may reach the QGP phase. The created matter quickly expands, cools down, and finally decays into hadrons. These decay products are measured in detectors surrounding the collision point.

The dependence of the early stage temperature  $T$  on the collision energy in the SMES is shown in Fig. 1, *a*. Outside the transition region,  $T$  increases with  $F$ . The Fermi's energy measure  $F$  is defined in Eq. (1). Inside the transition region,  $T$  is constant. The fraction of the volume occupied by the QGP at the early stage of an A+A central collision increases rapidly in the transition region, as shown in Fig. 1, *b*.

The majority of all particles produced in high energy interactions are pions. Thus, pions carry a basic information on the entropy created in the collisions. On the

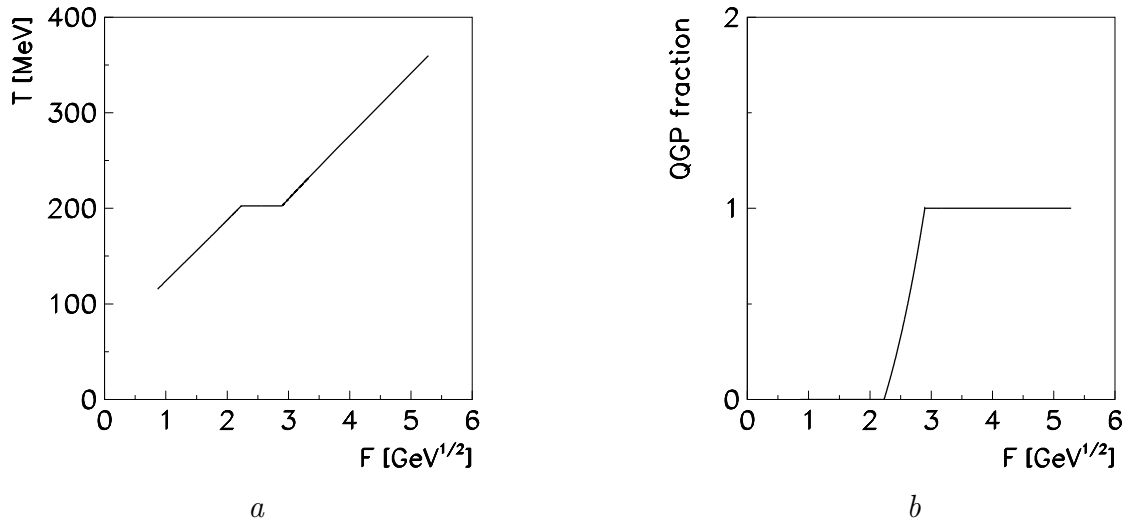


Fig. 1. (a): The early stage (initial) temperature of the fireball as a function of  $F$ . (b): The fraction of volume occupied by the QGP as a function of  $F$ .

other hand, the entropy production should depend on the form of matter present at the early stage of collisions. A deconfined matter is expected to lead to the final state with higher entropy than that created by a confined matter. Consequently, it is natural to expect that the onset of creation of a deconfined matter should be signalled by an enhancement of the pion production. The simple intuitive argumentation can be further quantified within SMES assuming the generalized Fermi–Landau initial conditions: the initial volume is Lorenz-contracted,  $V \propto \langle N_W \rangle (\sqrt{s_{NN}})^{-1}$ , where  $\sqrt{s_{NN}}$  is the c.m.s. energy of the nucleon pair and  $\langle N_W \rangle$  is the mean number of wounded nucleons (i.e. the number of nucleons participating in an A+A inelastic reaction). A trivial dependence of the pion multiplicity on the size of colliding nuclei should be removed, and, thus, a relevant observable is the ratio of the mean pion multiplicity  $\langle \pi \rangle$  to  $\langle N_W \rangle$ . The initial energy density is given by  $\varepsilon \propto gT^4 \propto (\sqrt{s_{NN}} - 2m_N) \sqrt{s_{NN}}$ , where  $g$  is the effective number of internal degrees of freedom at the early stage, and  $m_N$  is the nucleon mass. The pion multiplicity is proportional to the initial entropy, and the  $\langle \pi \rangle / \langle N_W \rangle$  ratio can be thus calculated outside the transition region as:

$$\frac{\langle \pi \rangle}{\langle N_W \rangle} \propto \frac{VgT^3}{\langle N_W \rangle} \propto \frac{g^{1/4} (\sqrt{s_{NN}} - 2m_N)^{3/4}}{(\sqrt{s_{NN}})^{1/4}} \equiv g^{1/4} F. \quad (1)$$

Therefore, the  $\langle \pi \rangle / \langle N_W \rangle$  ratio increases linearly with Fermi's energy measure  $F$  outside the transition region, and the slope parameter is proportional to  $g^{1/4}$  [7]. In the transition region, a steepening of the pion energy de-

pendence is predicted, because of the activation of partonic degrees of freedom, i.e., the effective number of internal degrees of freedom in QGP is larger than that in the hadron gas (HG):  $g_{\text{QGP}} > g_{\text{HG}}$ .

The compilation of data on the pion multiplicity in central Pb+Pb (Au+Au) collisions and  $p + p(\bar{p})$  interactions is shown in Fig. 2, *a*: the figure presents the data available as of 1998, and the *b* one shows presently available NA49 results [5]. In Fig. 2, *b*, the mean pion multiplicity  $\langle \pi \rangle = 1.5 (\langle \pi^- \rangle + \langle \pi^+ \rangle)$  per wounded nucleon is shown as a function of  $F$ . The results from  $p + p(\bar{p})$  interactions are shown by the open symbols. Up to the top SPS energy, the mean pion multiplicity in  $p + p$  interactions is approximately proportional to  $F$ . A fit of  $\langle \pi \rangle / \langle N_W \rangle = bF$  yields a value of  $b \cong 1.063 \text{ GeV}^{-1/2}$ . For central Pb+Pb and Au+Au collisions, the energy dependence is more complicated. Below 40 AGeV, the ratio  $\langle \pi \rangle / \langle N_W \rangle$  is lower in A+A collisions than that in  $p + p(\bar{p})$  interactions (pion suppression), while this ratio is larger at higher energies in A+A collisions than that in  $p + p(\bar{p})$  interactions (pion enhancement). A linear fit,  $\langle \pi \rangle / \langle N_W \rangle = a + bF$  for  $F < 1.85 \text{ GeV}^{1/2}$ , gives  $a \cong -0.45$  and  $b \cong 1.03 \text{ GeV}^{-1/2}$ . The slope parameter fitted in the range  $F > 3.5 \text{ GeV}^{1/2}$  is  $b \cong 1.33$ . This is shown by the solid line in Fig. 2 (the lowest point at the top RHIC energy was excluded from the fit). Thus, in the region 15–40 AGeV between the highest AGS and the lowest SPS energy, the slope increases by a factor of about 1.3. This increase of the slope for A+A collisions is interpreted within the SMES as due to an increase of the effective number of internal degrees of freedom by a

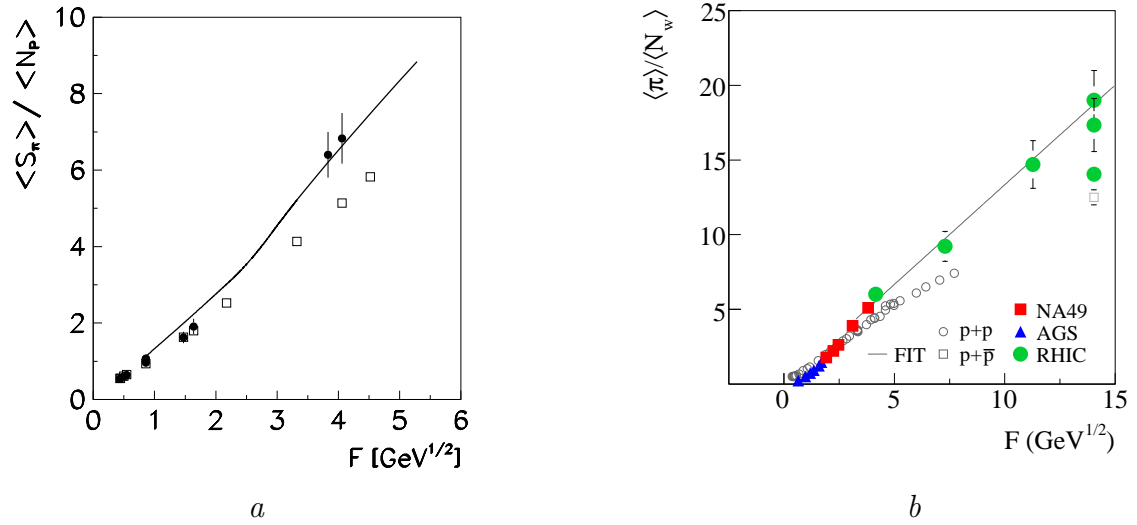


Fig. 2. (a): The  $\langle S_\pi \rangle / \langle N_p \rangle$  ratio as a function of  $F$ . Experimental data on central collisions of two identical nuclei are indicated by closed circles. The data correspond to the compilations existed as of 1998. They are compared with the SMES [4] shown by the solid line. The open boxes show results obtained for nucleon–nucleon interactions. (b): Energy dependence of the mean pion multiplicity per wounded nucleon measured in central Pb+Pb and Au+Au collisions (full symbols), compared to the corresponding results from  $p+p(\bar{p})$  reactions (open symbols). The compilation of data is from [5]

factor of  $g_{\text{QGP}}/g_{\text{HG}} = (1.3)^4 \cong 3$  [4, 7]. It is caused by the creation of a transient state of deconfined matter at collision energies higher than 30 AGeV.

### 3. Horn

The energy dependence of the strangeness-to-entropy ratio is a crucial signal of the deconfinement. The temperature dependence of a particle multiplicity is strongly dependent on the particle mass,

$$\langle N_i \rangle = \frac{g_i V}{2\pi^2} m_i^2 T K_2 \left( \frac{m_i}{T} \right), \quad (2)$$

where  $g_i$  and  $m_i$  are, respectively, the degeneracy factor and the particle mass, and  $K_2$  is the modified Hankel function. For light hadrons ( $m_l/T \ll 1$ ), one finds  $\langle N_l \rangle \propto T^3$  from Eq. (2), whereas, for heavy hadrons ( $m_h/T \gg 1$ ), Eq. (2) leads to  $\langle N_h \rangle \propto T^{3/2} \exp(-m_h/T)$ . Within SMES at low collision energies, when the HG matter is produced, the strangeness-to-entropy ratio steeply increases with the collision energy. This is due to a low temperature at the early stage and the high mass of the carriers of strangeness (the kaon mass), i.e.,  $m_K \gg T$ , and the total strangeness is proportional to  $T^{3/2} \exp(-m_K/T)$ . On the other hand, the total entropy is approximately proportional to  $T^3$ . Therefore, the strangeness-to-pion ratio is approximately  $T^{-3/2} \exp(-m_K/T)$  in the HG and strongly

increases with the collision energy. When the transition to a deconfined matter is crossed, the mass of the strangeness carriers is significantly reduced ( $m_s \cong 150$  MeV, the strange quark mass). Due to the low mass ( $m_s < T$ ), the strangeness yield becomes approximately proportional to the entropy (both are proportional to  $T^3$ ), and the strangeness-to-entropy (or pion) ratio becomes independent of the energy in the QGP. This leads to a “jump” in the energy dependence from the larger value for confined matter to a less value for deconfined matter. Thus, within the SMES, the non-monotonic energy dependence of the strangeness-to-entropy ratio is followed by a saturation at the deconfined value which is a direct consequence of the onset of deconfinement taking place at about 30 AGeV [4]. This is illustrated by Fig. 3.

One can argue that the strangeness-to-entropy ratio is closely proportional to the two ratios directly measured in experiments: the  $\langle K^+ \rangle / \langle \pi^+ \rangle$  ratio and the  $E_s = (\langle \Lambda \rangle + \langle K + \bar{K} \rangle) / \langle \pi \rangle$  ratio. The energy dependence of these full phase space ratios is plotted in Fig. 4 for central Pb+Pb (Au+Au) collisions and  $p+p$  interactions.

Kaons are the lightest strange hadrons, and  $\langle K^+ \rangle$  accounts for about a half of all the antistrange quarks produced in Pb+Pb collisions at AGS and SPS energies.  $K^+$  and  $K^0$  carry a dominant fraction of all produced  $\bar{s}$ -quarks exceeding 95% in Pb+Pb collisions at 158 AGeV

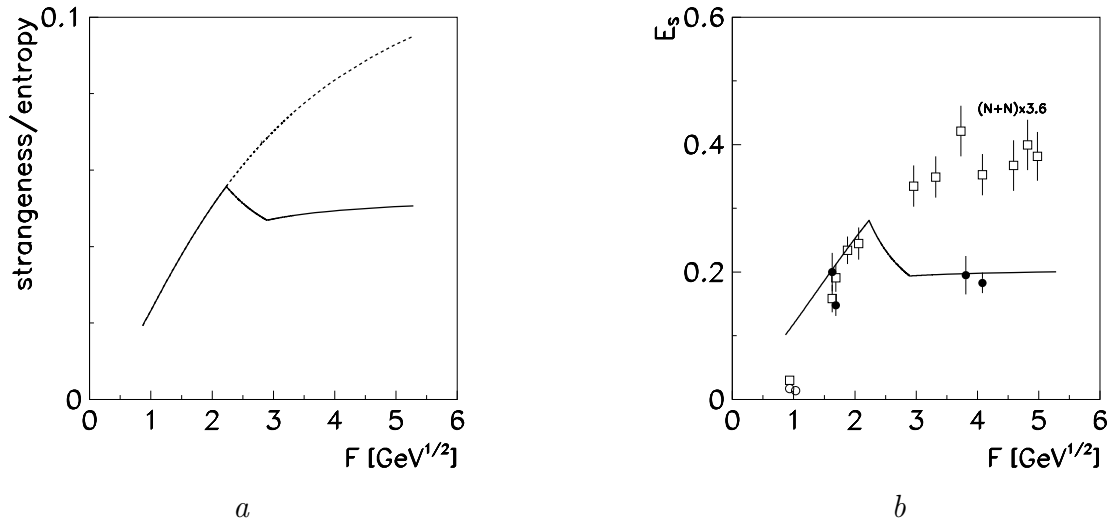


Fig. 3. (a): The ratio of the total number of  $s$  and  $\bar{s}$  quarks and antiquarks to the entropy (solid line) as a function of  $F$  [4]. The dashed line indicates the corresponding ratio calculated assuming the absence of the phase transition to the QGP. (b): The ratio  $E_s$  as a function of  $F$ . Experimental data on central collisions of two identical nuclei existed as of 1998 are indicated by closed circles. These data should be compared with the SMES predictions [4] shown by the solid line. The open boxes show results obtained for nucleon–nucleon interaction, scaled by a factor 3.6 to match A+A data at the AGS energy

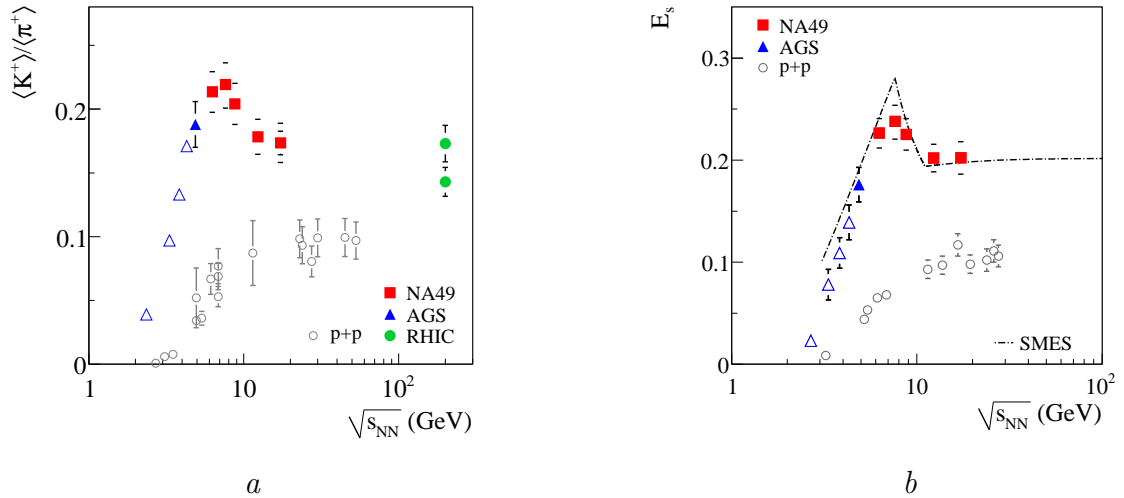


Fig. 4. (a): Energy dependence of the  $\langle K^+ \rangle / \langle \pi^+ \rangle$  ratio measured in central Pb+Pb and Au+Au collisions (full symbols) compared to the corresponding results from  $p+p$  reactions (open circles). (b): Energy dependence of the relative strangeness production as measured by the  $E_s$  ratio (see the text) in central Pb+Pb and Au+Au collisions (full symbols) compared to results from  $p+p$  reactions (open circles). The compilation of data is from [5]. The dash-dotted line shows the predictions of the SMES [4]

if open strangeness is considered. Because  $\langle K^+ \rangle \cong \langle K^0 \rangle$  in approximately isospin symmetric collisions of heavy nuclei, the  $K^+$  yield is nearly proportional to the total strangeness production and only weakly sensitive to the baryon density. As a significant fraction of  $s$ -quarks (about 50% in central Pb+Pb collisions at 158 A·GeV) is carried by hyperons, the number of produced antikaons,

$K^-$  and  $\bar{K}^0$ , is sensitive to both the strangeness yield and the baryon density. In the  $E_s$  ratio, all main carriers of strange and antistrange quarks are included. The neglected contribution of  $\bar{\Lambda}$  and other hyperons and antihyperons is about 10% at SPS energies. Both the  $\langle K^+ \rangle / \langle \pi^+ \rangle$  and  $E_s$  ratios are approximately, within 5% at SPS energies, proportional to the ratio of the total

multiplicity of  $s$  and  $\bar{s}$  quarks to the multiplicity of pions. It should be noted that the  $\langle K^+ \rangle / \langle \pi^+ \rangle$  ratio is expected to be similar (within about 10%) for  $p + p$ ,  $n + p$ , and  $n + n$  interactions at 158 AGeV, whereas the  $E_s$  ratio is independent of the isospin of nucleon-nucleon interactions.

For  $p + p$  interactions, both ratios show the monotonic increase with energy. However, the very different behavior is observed for central Pb+Pb (Au+Au) collisions. The steep threshold rise of the ratios characteristic of confined matter then settles into the saturation at the level expected for deconfined matter. In the transition region (at low SPS energies), a sharp maximum caused by a higher strangeness-to-entropy ratio in confined matter than that in deconfined matter is observed. As seen in Fig. 4, the measured dependence is consistent with that predicted within the SMES [4].

#### 4. Step

The energy density at the early stage increases with the collision energy. At low and high energies, when the pure confined or deconfined phase is produced, this leads to an increase of the initial temperature and pressure. This, in turn, results in an increase of the transverse expansion of a matter and, consequently, a flattening of the transverse mass spectra of final-state hadrons. One may expect an ‘anomaly’ [8–10] in the energy dependence of the transverse hadron activity as the temperature and the pressure are approximately constant in the mixed phase.

The experimental data on the transverse mass spectra are usually parametrized by a simple exponential dependence:

$$\frac{dN}{m_T dm_T} \propto \exp\left(-\frac{m_T}{T^*}\right), \quad (3)$$

where  $m_T = (m^2 + p_T^2)^{1/2}$ . The inverse slope parameter  $T^*$  is sensitive to both thermal and collective motions in the transverse direction. The hydrodynamic transverse flow with collective velocity  $v_T$  modifies the Boltzmann  $m_T$ -spectrum of hadrons. At low transverse momenta, it leads to the result ( $T_{\text{kin}}$  is a kinetic freeze-out temperature):  $T_{\text{low-}p_T}^* \cong T_{\text{kin}} + \frac{1}{2}m v_T^2$ . A linear mass dependence of  $T^*$  is supported by the data for hadron spectra at small  $p_T$ . However, for  $p_T \gg m$ , the hydrodynamic transverse flow leads to the mass-independent blue-shifted “temperature”:  $T_{\text{high-}p_T}^* = T_{\text{kin}} [(1+v_T)/(1-v_T)]^{1/2}$ . Note that a simple exponential fit (3) works neither for light  $\pi$ -mesons,  $T_{\text{low-}p_T}^*(\pi) < T_{\text{high-}p_T}^*(\pi)$ , nor for heavy (anti)protons

and (anti)lambdas,  $T_{\text{low-}p_T}^*(p, \Lambda) > T_{\text{high-}p_T}^*(p, \Lambda)$  (see e.g., [11, 12]).

Kaons are the best and unique particles among measured hadron species for observing the effect of a modification of the equation of state due to the onset of the deconfinement in hadron transverse momentum spectra. The arguments are the following [10]: 1) the kaon  $m_T$ -spectra are only weakly affected by the hadron re-scattering and resonance decays during the post-hydrodynamic hadron cascade at the SPS and RHIC energies; 2) a simple one-parameter exponential fit (3) is quite accurate for kaons in central A+A collisions at all energies, i.e.  $T_{\text{low-}p_T}^*(K) \approx T_{\text{high-}p_T}^*(K)$  for kaons; 3) the high-quality data on the  $m_T$ -spectra of  $K^+$  and  $K^-$  mesons in central Pb+Pb and Au+Au collisions are available in the full range of relevant energies. Thus, one expects [10] that  $T^*$  for kaons increases when either the pure confined or deconfined phase is produced at the early stage of A+A collisions, but  $T^*$  remains approximately constant when the initial matter is in a mixed phase state.

The energy dependence of the inverse slope parameter fitted to the  $K^+$  and  $K^-$  transverse mass spectra for central Pb+Pb (Au+Au) collisions is shown in Fig. 5.

The striking features of the data can be summarized and interpreted as follows. The  $T^*$  parameter increases strongly with the collision energy up to the SPS energy point of 30 AGeV. This is the energy region where the creation of confined matter at the early stage of the collisions is expected. Increasing the collision energy leads to an increase of the early stage temperature (see Fig. 1, a) and pressure. Consequently, the transverse activity of produced hadrons, measured by the inverse slope parameter, increases with the energy. The  $T^*$  parameter is approximately independent of the collision energy in the SPS energy range 30–158 AGeV. In this energy region, the transition between confined and deconfined matter is expected to be located. The resulting modification of the equation of state “suppresses” the hydrodynamic transverse expansion and leads to the observed plateau structure in the energy dependence of the  $T^*$  parameter [10, 13]. At higher energies (RHIC data),  $T^*$  again increases with the collision energy. The equation of state at the early stage becomes again stiff, the early stage temperature and pressure increase with the collision energy, and this results in an increase of  $T^*$  too. The parameter  $T^*$  appears to increase smoothly in  $p + p$  interactions, as shown in the left panel in Fig. 5.

For the transverse mass spectra of pions and protons, the inverse slope parameter depends on the transverse mass interval used in the fit. The mean transverse mass

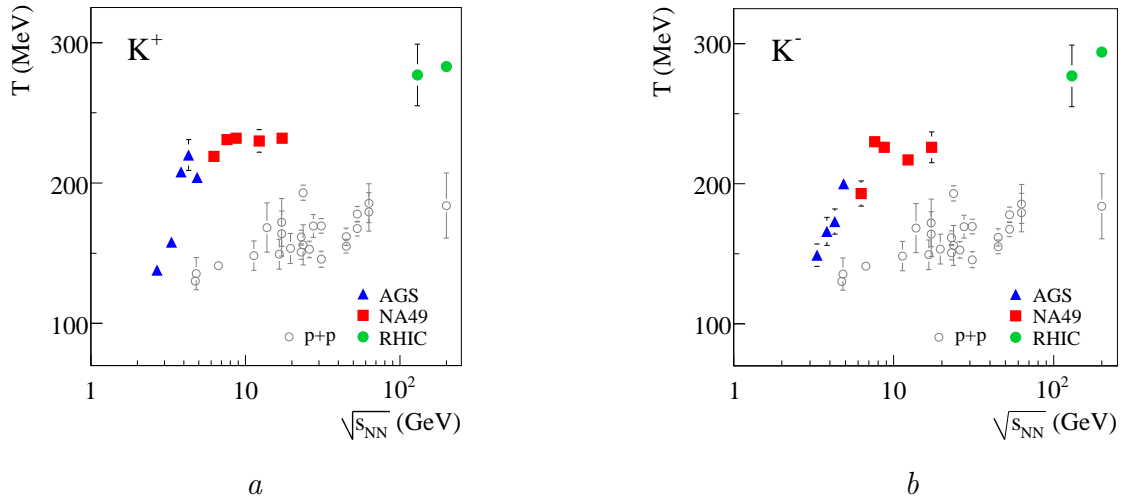


Fig. 5. Energy dependence of the inverse slope parameter  $T^*$  of the transverse mass spectra of  $K^+$  (a) and  $K^-$  mesons (b) measured at a mid-rapidity in central Pb+Pb and Au+Au collisions. The  $K^\pm$  slope parameters are compared to those from  $p+p$  reactions (open circles). The compilation of data is from [5]

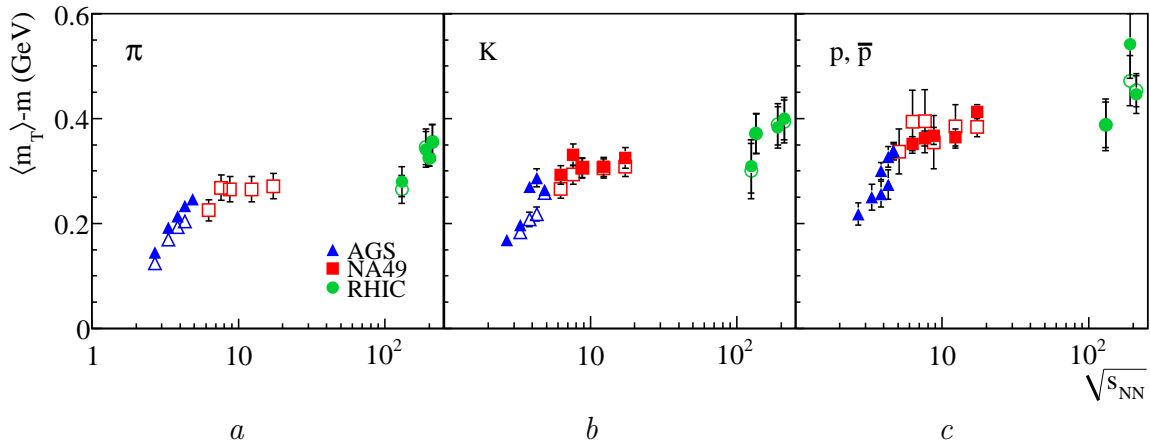


Fig. 6. The energy dependence of  $\langle m_T \rangle - m$  for  $\pi^\pm$  (a),  $K^\pm$  (b), and  $p$  and  $\bar{p}$  (c). In the plots, positively (negatively) charged hadrons are indicated by the full (open) symbols. The compilation of data is from [5]

$\langle m_T \rangle$  provides an alternative characterization of the  $m_T$ -spectra. The energy dependence of  $\langle m_T \rangle - m$  for pions, kaons, and (anti)protons is shown in Fig. 6. The results shown in Fig. 6 demonstrate that the approximate energy independence of  $\langle m_T \rangle$  in the SPS energy range is a common feature for all particles under study.

## 5. Longitudinal Collective Flow

The collective flow of matter at the freeze-out depends on the properties of the early stage, as well as on the expansion dynamics itself. Within the SMES, the collision energy dependence of the early stage properties is predicted. In particular, in the energy range in which the

mixed phase is created, the pressure and the temperature are constant, and, at the end of the mixed phase domain, the pressure-to-energy density ratio reaches its minimum (the softest point of the EoS). From general hydrodynamic considerations, this is expected to lead to a reduction of the buildup of the transverse flow [10]. Similar effects are seen for the longitudinal collective flow [14] within Landau's hydrodynamic model [15, 16]. The interest in this model was revived by the remarkable observation that the rapidity distributions at all investigated energies can be well described by a single Gaussian (see [17] and references therein). Moreover, the energy dependence of the width can also be described reasonably well by the same model.

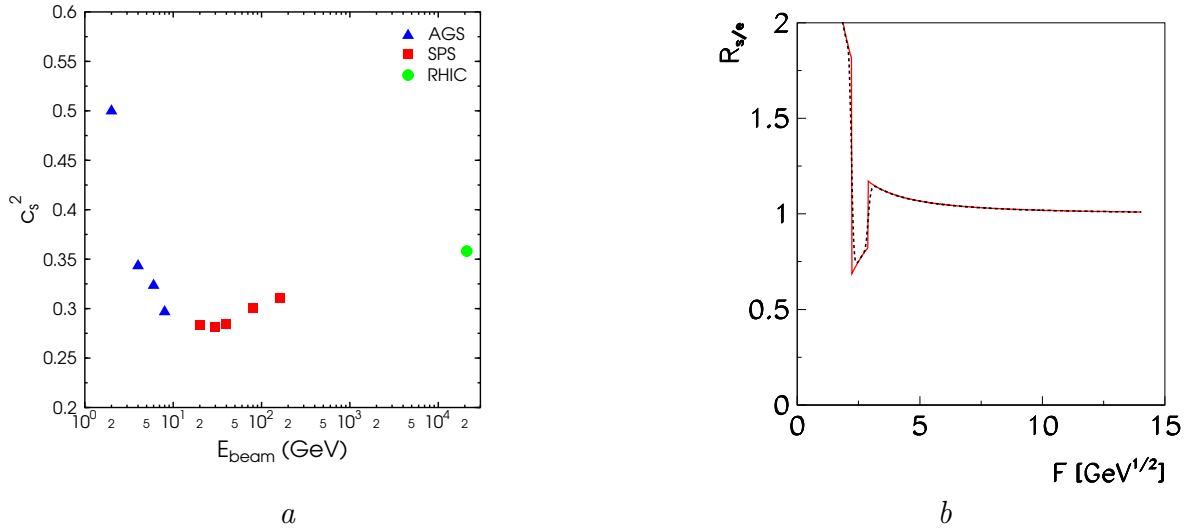


Fig. 7. (a): Speed of sound as a function of the beam energy for central Pb+Pb (Au+Au) reactions as extracted from the data using Eq. (6) [14]. (b): The *tooth* structure in the ratio of strangeness and entropy fluctuations  $R_{s/e}$  (9) (see [19])

The main physics assumptions of Landau's picture are as follows. The collision of two Lorentz-contracted nuclei leads to a complete stopping of the colliding nuclei and the full thermalization of the created hadronic matter. This establishes the volume and the energy density for the initial conditions of the hydrodynamic expansion at each collision energy. Assuming, for simplicity, the equation of state in the form  $p = c_s^2 \varepsilon$  (where  $p$  and  $\varepsilon$  correspond to the pressure and the energy density, respectively, and  $c_s$  denotes the speed of sound, with  $c_s^2 = 1/3$  for an ideal massless particle gas), the pion rapidity spectrum is given by

$$\frac{dn}{dy} = \frac{K s_{NN}^{1/4}}{\sqrt{2\pi\sigma_y^2}} \exp\left(-\frac{y^2}{2\sigma_y^2}\right) \quad (4)$$

with

$$\sigma_y^2 = \frac{8}{3} \frac{c_s^2}{1 - c_s^4} \ln(\sqrt{s_{NN}}/2m_N), \quad (5)$$

where  $K$  is a normalization factor converting the entropy to the pion density<sup>1</sup>.

Equations (4)–(5) with  $c_0^2 = 1/3$  only roughly reproduce the measured dependence of  $\sigma_y^2$  on the collision energy. At low AGS energies and at the top RHIC energy, the experimental points are underpredicted, while,

in the SPS energy range, Landau's model overpredicts the width of the rapidity distributions. These deviations can be attributed to changes in the equation of state, which can be effectively parametrized by allowing the speed of sound to be dependent on the collision energy. By inverting Eq. (5), one can express  $c_s^2$  as a function of the measured width of the rapidity distribution:

$$c_s^2 = \sqrt{\left[\frac{4\ln(\sqrt{s_{NN}}/2m_N)}{3\sigma_y^2}\right]^2 + 1} - \frac{4\ln(\sqrt{s_{NN}}/2m_N)}{3\sigma_y^2}. \quad (6)$$

The energy dependence of the sound velocities extracted from the data using Eq. (6) is presented in Fig. 7, a. The sound velocities exhibit a clear minimum (usually called the softest point) around a beam energy of  $\sqrt{s_{NN}} = 7.6$  GeV (30 AGeV). As discussed previously, the weakening of the transverse and longitudinal expansions is expected within the SMES at low SPS energies due to the onset of deconfinement, which softens the EoS at the early stage. Generally, a softening of the equation of state was predicted as a signal for the mixed phase at the transition energy from hadronic to partonic matter. Therefore, we conclude that the data on rapidity spectra of negatively charged pions are indeed compatible with the assumption of the onset of deconfinement at the low SPS energies.

<sup>1</sup> Note that Eq. (5) is obtained, by assuming that  $c_s$  depends only on the early-stage energy density, and its dependence on the decreasing energy density during the expansion is neglected. This assumption needs the clarification in the future studies

## 6. Event-by-Event Fluctuations

Up to this point, only the quantities averaged over many collisions (events) were considered. Next, an extension of the SMES, which leads to predictions of fluctuations from event to event, is reviewed. The key additional assumption is that even if the collision energy is fixed, the energy used for the particle production (inelastic energy) can still fluctuate. These dynamical energy fluctuations lead to dynamical fluctuations of macroscopic properties  $X$  of the matter, like its entropy and strangeness content. The relation between them is given by the EoS. For example, different values of the energy of the early equilibrium state lead to different, but uniquely determined, entropies. Since the EoS shows an anomalous behavior in the phase transition region, this anomaly should also be visible in the ratio of entropy to energy fluctuations [18].

According to the first and second principles of thermodynamics, the entropy change  $\delta S$  is given as  $T\delta S = \delta E + p\delta V$ . For central A+A collisions, one expects  $\delta V \cong 0$ . Within the SMES, the ratio of entropy to energy fluctuations can then be calculated and expressed as a simple function of the  $p/\varepsilon$  ratio [18]:

$$R_e \equiv \frac{(\delta S)^2/S^2}{(\delta E)^2/E^2} = \left(1 + \frac{p}{\varepsilon}\right)^{-2}. \quad (7)$$

Within the SMES model, the confined matter (which is modeled as an ideal gas) is created at the early collision stage below a collision energy of  $30A$  GeV. In this domain, the ratio  $p/\varepsilon$  and, consequently, the  $R_e$  ratio are approximately independent of the collision energy and equal about  $1/3$  and  $0.56$ , respectively. The SMES model assumes that the deconfinement phase transition is of the first order. Thus, there is a mixed phase region corresponding to the energy interval  $30A$ – $60A$  GeV. At the end of this region, the  $p/\varepsilon$  ratio reaches a minimum (the “softest point” of the EoS). Thus, in the transition energy range, the  $R_e$  ratio increases and reaches its maximum,  $R_e \approx 0.8$ , at the end of the transition domain. Further on, in the pure deconfined phase, which is represented by the ideal quark-gluon gas at a bag pressure, the  $p/\varepsilon$  ratio increases and again approaches its asymptotic value  $1/3$  at the highest SPS energy of  $160A$  GeV. The early stage energy and entropy fluctuations entering Eq. (7) are not directly observable. However, as argued in [18], they can be inferred from the experimentally accessible information on the final state energy and multiplicity fluctuations.

In [19], the energy dependence of dynamical strangeness fluctuations caused by dynamical energy

fluctuations was studied within the SMES model. Defining  $\bar{N}_s$  as the total number of strange quark–antiquark pairs created in an A+A collision, one calculates the fluctuation ratio as

$$R_s = \frac{(\delta \bar{N}_s)^2/\bar{N}_s^2}{(\delta E)^2/E^2}. \quad (8)$$

For  $T \rightarrow \infty$ , the system is in the QGP phase. Strange (anti)quarks can be considered as massless, and the bag constant can be neglected. Then  $\varepsilon \propto T^4$  and  $n_s \propto T^3$  and, consequently,  $d\varepsilon/\varepsilon = 4dT/T$  and  $dn_s/n_s = 3dT/T$ , which results in  $R_s = (3/4)^2 \cong 0.56$ . In the confined phase,  $T < T_c$ , the energy density is still approximately proportional to  $T^4$  due to the dominant contributions of non-strange hadron constituents. However, the dependence of the strangeness density on  $T$  is governed by the exponential factor,  $n_s \propto \exp(-m_S/T)$ , as  $T \ll m_S = m_W^s \cong 500$  MeV. Therefore, at small  $T$ , one finds  $d\varepsilon/\varepsilon = 4dT/T$  and  $dn_s/n_s = m_S dT/T^2$ , so that the ratio  $R_s = m_S/(4T)$  decreases with  $T$ . The strangeness density  $n_s$  is small and goes to zero as  $T \rightarrow 0$ , but the fluctuation ratio  $R_s$ , Eq. (8), is large and increases to infinity in the zero temperature limit. One finds a non-monotonic energy dependence of  $R_e$  with a maximum at the boundary between the mixed phase and the QGP [18]. A pronounced minimum-structure is expected in the dependence of  $R_s$  on the collision energy [19]. It is located at  $\sqrt{s_{NN}} = 7$ – $12$  GeV ( $30$ – $60$  AGeV), where the mixed phase is created at the early stage of A+A collisions.

Both entropy and strangeness fluctuation measures,  $R_e$  and  $R_s$ , show the anomalous behavior in the transition region: a maximum is expected for  $R_e$  and a minimum for  $R_s$ . Consequently, an even stronger anomaly is predicted for the ratio

$$R_{s/e} \equiv \frac{R_s}{R_e} = \frac{(\delta \bar{N}_s)^2/\bar{N}_s^2}{(\delta \bar{N}_-)^2/\bar{N}_-^2} \quad (9)$$

shown in Fig. 7, *b*. Experimental measurements of  $R_{s/e}$  may be easier than those of  $R_e$  and  $R_s$ , because the ratio  $R_{s/e}$  requires measurements of particle multiplicities only, whereas both  $R_e$  and  $R_s$  involve also measurements of particle energies.

The *tooth* structure in the energy dependence of  $R_{s/e}$  shown in Fig. 7, *b* might be seen in the event-by-event fluctuations of the  $K/\pi$  ratio. The energy dependence of the fluctuations of this ratio in central Pb+Pb collisions was studied by NA49 using the so-called  $\sigma_{dyn}$  measure [20]. The “dynamical”  $K/\pi$  fluctuations increase significantly, as the energy decreases below  $40A$  GeV. However,

it is unclear whether this increase is related to the rapid increase of the  $R_{s/e}$  measure predicted due to the onset of deconfinement at energies below 30 AGeV.

## 7. Conclusions

In this review, we present the experimental and theoretical status of the evidence of the threshold of quark-gluon plasma creation in high-energy nucleus-nucleus interactions. The location of this so-called onset of deconfinement in energy, as well as key experimental signals, was predicted by the statistical model of the early stage of the collision process [4]. These signals were searched for and observed within the energy scan program of the NA49 Collaboration at the CERN SPS. Together with measurements at lower (LBL, JINR, SIS, BNL AGS) and higher (BNL RHIC) energies, the properties of hadron production in heavy ion collisions were established in a broad energy range. Their energy dependence led to the conclusion that the predicted signals of the onset of deconfinement appear in a common energy domain covered by the SPS at CERN. These features of the data serve as a strong experimental evidence of the existence of the onset of deconfinement and thus of the quark-gluon plasma itself. The anomalies in the energy dependence of the hadron production are seen in nucleus-nucleus collisions and absent in the data of  $p + p$  reactions. They indicate that the onset of the deconfinement in central Pb+Pb collisions is located at about 30 AGeV.

New experimental programs have started at the CERN SPS and BNL RHIC and are devoted to the study of nucleus-nucleus collisions in the energy region, where the NA49 experiment found the evidence of the onset of deconfinement. The STAR experiment at RHIC will provide a necessary confirmation of these results. The new CERN experiment NA61 will address the questions how this observed phenomenon depends on the volume of matter and which properties of the transition region are.

I am grateful to Marek Gaździcki for the fruitful collaboration. I also thank Walter Greiner for his permanent support and encouraging of these studies. This work was supported in part by the Program of Fundamental Research of the Division of Physics and Astronomy of the NAS of Ukraine.

1. D.D. Ivanenko and D.F. Kurdgelaidze, *Astrophysics* **1**, 251 (1965).

2. N. Cabibbo and G. Parisi, *Phys. Lett. B* **59**, 67 (1975), J.C. Collins and M.J. Perry, *Phys. Rev. Lett.* **34**, 1353 (1975).
3. E.V. Shuryak, *Phys. Rept.* **61**, 71 (1980).
4. M. Gaździcki and M.I. Gorenstein, *Acta Phys. Polon. B* **30**, 2705 (1999).
5. C. Alt *et al.* [NA49 Collaboration], *Phys. Rev. C* **77**, 024903 (2008).
6. M. Gaździcki, M.I. Gorenstein, and P. Seyboth, arXiv:1006.1765 (2010).
7. M. Gaździcki, *Z. Phys. C* **66**, 659 (1995); *J. Phys. G* **23**, 1881 (1997).
8. L. Van Hove, *Phys. Lett. B* **118**, 138 (1982).
9. C.M. Hung and E. Shuryak, *Phys. Rev. Lett.* **75**, 4003 (1995); *Phys. Rev.* **57**, 1891 (1997).
10. M.I. Gorenstein, M. Gaździcki, and K. Bugaev, *Phys. Lett. B* **567**, 175 (2003).
11. D. Teaney, J. Lauret, and E.V. Shuryak, *Phys. Rev. Lett.* **86**, 4783 (2001).
12. M.I. Gorenstein, K. Bugaev, and M. Gaździcki, *Phys. Rev. Lett.* **88**, 132301 (2002); *Phys. Lett. B* **544**, 127 (2002); *Phys. Rev. C* **68**, 01790 (2003).
13. M. Gaździcki, M.I. Gorenstein, F. Grassi, Y. Hama, T. Kodama, and O. Socolowski jr., *Braz. J. Phys.* **34**, 322 (2004); Y. Hama, F. Grassi, O. Socolowski, T. Kodama, M. Gaździcki, and M. Gorenstein, *Acta Phys. Polon. B* **35**, 179 (2004).
14. M. Bleicher, arXiv:hep-ph/0509314.
15. L.D. Landau, *Izv. Akad. Nauk Ser. Fiz.* **17**, 51 (1953).
16. S.Z. Belenkij and L.D. Landau, *Nuovo Cim. Suppl.* **3S10**, 15 (1956) [*Usp. Fiz. Nauk* **56**, 309 (1955)].
17. C. Alt *et al.* [NA49 Collaboration], *Phys. Rev. C* **79**, 044910 (2009).
18. M. Gaździcki, M.I. Gorenstein, and S. Mrowczynski, *Phys. Lett. B* **585**, 115 (2004).
19. M.I. Gorenstein, M. Gaździcki, and O.S. Zozulya, *Phys. Lett. B* **585**, 237 (2004).
20. C. Alt *et al.* [NA49 Collaboration], *Phys. Rev. C* **79**, 044910 (2009).

Received 01.03.11

ДЕКОНФАЙНМЕНТ КВАРКІВ І ГЛЮОНІВ  
У ЯДРО-ЯДЕРНИХ ЗІТКНЕННЯХ

Марк І. Горештейн

Р е з ю м е

Енергетична залежність народження адронів у релятивістських ядро-ядерних зіткненнях демонструє декілька аномалій.

Ці аномалії були передбачені як сигнали фазового перетворення деконфайнмента, а потім підтверженні в експериментах по Pb+Pb зіткненням колаборацією NA49 у ЦЕРНі на при-

скорювачі SPS. Початок деконфайнмента у центральних ядроядерних зіткненнях має місце при енергії приблизно рівній 30 АГев.